THE EFFECT OF PRE-IMPACT SPIN ON THE MOON-FORMING COLLISION. S. Ruiz-Bonilla[1], V. R. Eke[1], J. A. Kegerreis[1], R. J. Massey[1], L. F. A. Teodoro[2, 3], [1]Institute for Computational Cosmology, Durham University, Durham, UK; [2]BAERI/NASA Ames Research Center, CA, USA; [3]School of Physics and Astronomy, University of Glasgow, Scotland, UK. *sergio.ruiz-bonilla@durham.ac.uk

Introduction: The final stage of planet formation involves giant impacts between planet-sized bodies [1]. Pre-impact spins are usually ignored despite the fact that rapidly rotating bodies are a common outcome of such collisions [2]. The main reasons being that the parameter space becomes huge, and spins make initial conditions tricky to construct. Examples of initial spins being ignored include attempts to explain Uranus' rotation axis [3, 4], and models in which the angular momentum of the Earth–Moon system results from the impact of a non-rotating Mars-sized body, Theia, and a non-rotating proto-Earth [5]. In this work, we show the importance of Theia´s spin in affecting the resulting debris disk from the Moon forming collision [6].

The Moon-forming impact is one planetary example for which pre-impact spin of the target alone has received limited consideration. Canup [7] showed how this changed the collision outcome relative to the canonical impact studied by Canup & Asphaug [6]. The isotopic similarity of the Earth's mantle and lunar samples [8] provoked attempts to place a higher fraction of proto-Earth material into the protolunar disc by starting with a spinning target [9, 10, 11]. Initial conditions for these numerical simulation studies were created by first making a spherical planet, providing it with a small angular velocity, letting it relax in a smoothed particle hydrodynamical (SPH) simulation, and then repeating this process until the desired angular velocity was reached [9]. This method is slow and leads to pre-impact planets with structures that cannot be known until the end of this iterative process.

We have developed a fast algorithm that calculates the internal density profile of a rotating object composed of any prescribed materials in hydrostatic equilibrium and places particles into the body such that very little, if any, relaxation is required for numerical simulations [6]. The method is based on the Concentric Maclaurin Spheroid (CMS) technique introduced by Hubbard [12] without differential rotation, but allowing arbitrary equations of state to be used for multiple materials. Our open-source code is a flexible tool that has been written in python under the project name WoMa (World Maker), and is publicly available at https://github.com/srbonilla/WoMa. We performed tests of our method for 1 and 2-layer planets with 10^5, 10^7, and 10^9 particles. The final density profiles, excluding the boundaries, are within 2 per cent of the desired, analytically computed density for the one- and two-layer tests with 10^5 particles, and within 1 per cent for the two higher resolutions. We use WoMa to construct initial conditions for a set of giant impacts between the proto-Earth and Mars-sized impactors with a variety of rotation rates.

The Effects of a Spinning Theia: We present a set of five canonical Moon-forming giant impacts where the impactor Theia is given a different spin in each simulation. We use the SWIFT open-source simulation code (www.swiftsim.com, [13]) version 0.8.1 for our SPH simulations.

We consider an impact between a target proto-Earth of mass 0.887 $M_\oplus$ and an impactor, Theia, of mass 0.133 $M_\oplus$. Both are differentiated into an iron core and rocky mantle, constituting 30 per cent and 70 per cent of the total mass, respectively, modelled using the Tillotson [14] iron and granite equations of state. The velocity at impact is chosen to be the mutual escape speed, the angle of impact is set as 45°, and the simulation begins 1 h prior to the time of contact between the two bodies in order to model the tidal distortion of the bodies just before impact. All five simulations are evolved to 100 h and have a mass resolution of 10^7 particles per Earth mass.

The only difference between our simulations is the rotation rate of Theia. The minimum period available is 2.6 h, which translates to a maximum spin angular momentum of $L_{Th,max} = 0.15\ L_{EM}$, where $L_{EM} = 3.5 \times 10^{34}$ kg m^2 s^{-1} is the current angular momentum of the Earth–Moon system. We set the spin angular momentum of Theia, L_{Th}, to be $l_{Th} \equiv L_{Th} / L_{Th,max} = -1/2$, $-1/4$, 0, 1/4, and 1/2 for our five simulations. These correspond to rotation periods for the more and less rapidly spinning Theias of 3.2 and 5.1 h. The orbital angular momentum of the colliding systems is 1.25 L_{EM}.

All counter-rotating ($l_{Th} < 1/2$) simulations place the majority of the mass of Theia either into the Earth or within the Roche radius ($\sim 3\ R_\oplus$), with much of Theia's core blanketing that of the proto-Earth. However, the $l_{Th} = 0$ and $l_{Th} = 1/2$ impacts lead to an approximately Moon-mass, self-gravitating clump within the debris disc whose periapsis is outside the Roche radius.

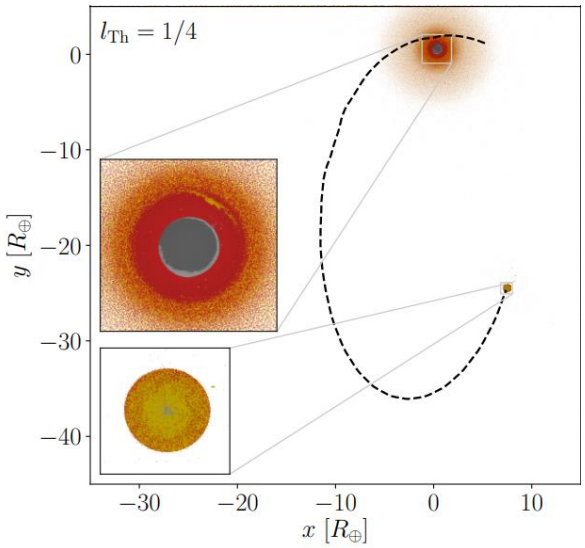

Figure 1: Snapshot at 100 h of simulation time for the simulation with $l_{\rm Th} = 1/4$. The black dashed line represents the trajectory of the resulting clump. The particle colours represent different materials: dark and light grey for iron, and red and yellow are rock, in the proto-Earth and Theia, respectively. An animation of the early evolution of all impacts is available at http://icc.dur.ac.uk/giant_impacts/woma_impacts_anim.mp4.

The orbiting clump is resolved with over 10^5 particles in the $l_{\rm Th} = 0$ and $l_{\rm Th} = 1/2$ simulations, allowing us to study in detail its composition. Both clumps have ∼29% of their mass coming from the proto-Earth's mantle, ∼1% from Theia's iron core, and the remaining ∼70% from Theia's mantle.

Fig. 2 shows how the mass fraction of proto-Earth increases linearly towards the surface of the clump. Roughly equal amounts of Theia and proto-Earth are found at the surface of the clump, quite different from the overall 70:30 split. This distribution of material is primarily a result of the geometry of the impact. Any long-term evolution of this distribution over time, due to convection and other mixing mechanisms, is not considered here. However, if subsequent mixing between proto-Earth and Theia material were incomplete, then this radial variation could establish a relation between the isotopic difference between these two bodies and that measured between the Earth and the Moon. The challenge of interpreting oxygen isotope data means that there is an ongoing debate as to whether the isotopic compositions of lunar samples and the Earth are indistinguishable [15] or not [16, 17, 18].

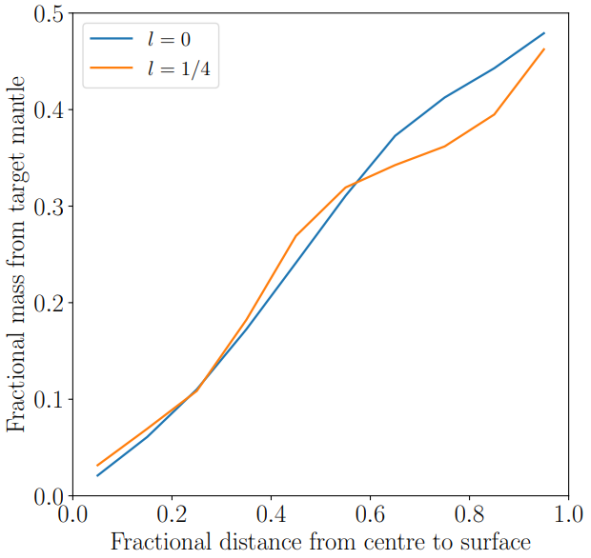

Figure 2: Radial variation of the mass fraction of target mantle present in the orbiting clumps after 100 h for the $l_{\rm Th} = 0$ (blue) and $l_{\rm Th} = 1/2$ (orange) simulations.

Conclusions: We developed a fast method to represent a spinning planet in a SPH simulation, publicly available at: https://github.com/srbonilla/WoMa. We tested its capabilities using simulations containing up to just over 10^9 SPH particles that were evolved with the SWIFT code.

We used this new technique to study the effect of different rotation rates of Theia in 10^7-particle simulations of a canonical Moon-forming impact. Counter-rotating Theias produced quick mergers, whereas a rapidly corotating Theia led to a hit-and-run collision with numerous unbound clumps escaping from the Earth. In the zero spin and slowly corotating Theia cases, after 100 h a roughly Moon-sized clump remained, orbiting the Earth outside the Roche radius.

References: [1] Chambers J. E. and Wetherill G. W. (1998) *Icarus, 136*, 304. [2] Kokubo E. and Genda H. (2010) *ApJ, 714*, L21. [3] Slattery W. L. et al. (1992) *Icarus, 99*, 167. [4] Kegerreis J. A. et al. (2018) *ApJ, 861*, 52. [5] Canup R. M. and Asphaug E. (2001) *Nature, 412*, 708. [6] Ruiz-Bonilla et al. (2021) *MNRAS 500*, 2861. [7] Canup R. (2008) *Icarus, 196*, 518. [8] Wiechert U. et al. (2001) *Science, 294*, 345. [9] Ćuk M. and Stewart S. T. (2012) *Science, 338*, 1047. [10] Lock S. J. and Stewart S. T. (2017) *J. Geophys. Res. (Planets), 122*, 950. [11] Wyatt B. M. et al. (2018), *JA&A, 39*, 26. [12] Hubbard W. B. (2013) *ApJ, 768*, 43. [13] Schaller M. et al. (2016) *Proc. PASC 16*. pp. 2:1–2:10. [14] Tillotson J. H. (1962) *General Atomic Report GA-3216*, 3216. [15] Young E. D. et al. (2016) *Science, 351*, 493. [16] Herwartz D. et al. (2014) *Science, 344*, 1146. [17] Greenwood R. C. et al. (2018) *Science Advances, 4*. [18] Cano E. J. et al. (2020) *Nature Geosci., 13*, 270.